JACS
JOURNAL OF THE AMERICAN CHEMICAL SOCIETY
Article
pubs.acs.org/JACS

Bis-1,3-dipolar Cycloadditions on Endohedral Fullerenes $M_3N@I_h$-C_{80} (M = Sc, Lu): Remarkable Endohedral-Cluster Regiochemical Control

Maira R. Cerón,[†] Marta Izquierdo,[†,∥,⊥] Marc Garcia-Borràs,[‡,⊥] Sarah S. Lee,[†] Steven Stevenson,[§] Sílvia Osuna,*[,‡] and Luis Echegoyen*[,†]

[†]Department of Chemistry, University of Texas at El Paso, 500 West University Avenue, El Paso, Texas 79968, United States
[‡]Institut de Química Computacional i Catàlisi (IQCC) and Departament de Química, Universitat de Girona, Campus Montilivi, Facultat de Ciències, 17071 Girona, Spain
[§]Department of Chemistry, Indiana-Purdue University at Fort Wayne, 2101 East Coliseum Boulevard, Fort Wayne, Indiana 46805, United States

Supporting Information

ABSTRACT: In this work, we briefly report some attempts to control regioisomeric bisadditions on $Sc_3N@I_h$-C_{80} and $Lu_3N@I_h$-C_{80} using the tether-controlled multifunctionalization method. We then describe the use of independent (nontethered) bis-1,3-dipolar cycloaddition reactions and the characterization of 5 new bisadducts, 3 for $Sc_3N@C_{80}$ and 2 for $Lu_3N@C_{80}$, which have never been reported before. Unexpectedly and remarkably, 4 of these compounds exhibit relatively high symmetry and 2 of these bisadducts are the first examples of intrinsically chiral endohedral compounds, due to the addition pattern, not to the presence of chiral centers on the addends. Since an analysis of the statistically possible number of bisadduct isomers on an I_h-C_{80} cage has not been reported, we present it here.

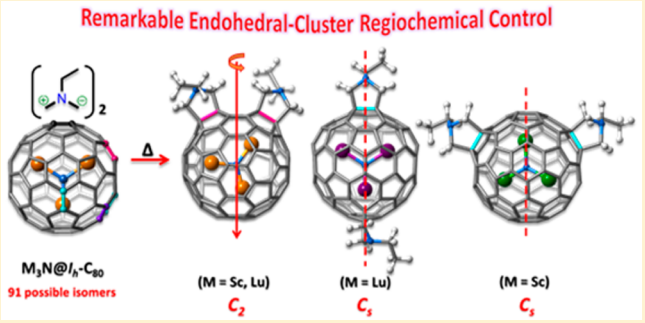

INTRODUCTION

In 1985, Kroto et al. discovered the fullerenes, which constituted new allotropic forms of carbon.[1] Since the early days of fullerene research, it was shown that they were capable of encapsulating atoms in their interior,[2] and these compounds were collectively denoted as endohedral fullerenes (EFs).[3] Endohedral fullerenes can also encapsulate small molecules,[4,5] one or more metals,[2] and metallic-based clusters.[6,7] Our recent work has been mainly focused on the trimetallic nitride cluster endohedral metallofullerenes (TNT-EMFs), initially discovered by Stevenson et al. in 1999 when they isolated $Sc_3N@I_h$-C_{80}.[8] These compounds exhibit considerable charge transfer from the trapped cluster to the carbon cage, formally represented as a six electron transfer leading to $[Sc_3N]^{6+}[C_{80}]^{6-}$.[9]

Since the first functionalization of EMFs in 1995 by Akasaka,[10] many have explored their reactivities and other properties,[11−13] allowing their characterization and enhancing their potential applications in biomedicine (as MRI contrast agents, in tumor diagnosis and radioimmunotherapy), in materials science and in photovoltaics solar cells, among others.[14,15] However, the complete structural, chemical and electronic properties of EMFs are not totally understood at the present time. Specifically, the factors controlling the regiochemistry of multiple additions to EFs remain largely unexplored and poorly understood.[16]

Multiple functionalizations of empty fullerenes have led to compounds that are very active as acceptors in organic photovoltaic (OPV) solar cells.[17−20] Controlling and understanding the formation of specific regioisomers of fullerene derivatives is important, because it has been shown that some regioisomerically pure fullerene bisadducts perform better in OPV solar cell devices than their corresponding isomeric mixtures.[21,22] There are very few methods available to regiochemically control bisadditions to fullerenes,[23,24] and the most widely utilized one is the tether-controlled remote multifunctionalization.[25,26] Since this method is extremely useful with [60]-fullerene and [70]-fullerene,[27−29] we decided to use it to control regiochemical bisadditions to $Sc_3N@I_h$-C_{80} and $Lu_3N@I_h$-C_{80}.

Independent (nontethered) bisadditions to endohedral fullerenes have been reported before, but very few details about their regiochemistry have been discussed.[30−35] Yamakoshi et al. reported regioselective bis-1,3-dipolar cycloaddition reactions using $M_3N@I_h$-C_{80} (M = Y and Gd) and described one predominant and unsymmetrical bispyrrolidine isomer, presumably controlled by the encapsulated cluster.[16] However, structural details were somewhat limited.

Received: July 10, 2015
Published: August 26, 2015

DOI: 10.1021/jacs.5b07207
J. Am. Chem. Soc. 2015, 137, 11775−11782

In this work, we briefly report some attempts to control regioisomeric bisadditions on $Sc_3N@I_h$-C_{80} and $Lu_3N@I_h$-C_{80} using the tether-controlled multifunctionalization method. We then describe the use of independent (nontethered) bis-1,3-dipolar cycloadditions and the characterization of 5 new bisadducts: 3 for $Sc_3N@C_{80}$ and 2 for $Lu_3N@C_{80}$.

RESULTS AND DISCUSSION

Tethered Bisadditions. We initially tried the following tether-controlled bisaddition reactions on $M_3N@I_h$-C_{80} (M = Sc and Lu): (a) a bis-1,3-dipolar cycloaddition reaction using phthaldehyde and *N*-ethyl glycine;[27] (b) a bisdiazo cyclopropanation reaction using 1,3-dibenzoylpropane-bis-*p*-toluenesulfonyl hydrazone;[36] and (c) a bis-Bingel cyclopropanation reaction using 1,3- phenylenedimethyl-diethylmalonate (PDM),[25] all of which are known to work efficiently on C_{60} and C_{70}.[25,27,29]

Remarkably, all of these reactions failed completely when applied to $M_3N@I_h$-C_{80} (M = Sc and Lu). MALDI and NMR techniques showed that none of the tethered bisadduct led to detectable amounts of the expected bisderivatives. Instead, monoadditions were observed in all cases. The obvious implication derived from these results is that the clusters must exert a very strong directing effect that prevents the addition of the second adduct, which is primarily directed by the tether length. Since Yamakoshi et al. were also unsuccessful at preparing isolable amounts of nontethered bisadducts of $M_3N@I_h$-C_{80} (M = Sc and Lu), we wondered if these specific TNT-EMFs were intrinsically unreactive toward bisadditions in general. To investigate this behavior, we decided to attempt the independent (nontethered) bis-1,3-dipolar cycloadditions on $M_3N@I_h$-C_{80} (M = Sc and Lu).

General Considerations. I_h-C_{80} endohedral fullerenes possess two different types of double bond addition sites: [6,6]-junctions (bonds between two six-membered rings) and [5,6]-junctions (bonds between one five membered ring and one six membered ring). Mono-additions of *N*-ethylazomethine ylides to I_h-C_{80} endohedral fullerenes have been shown to result in [5,6] or [6,6] fulleropyrrolidines.[37−39] The addition position of the monopyrrolidine adducts is strongly influenced by the size of the encapsulated cluster.[37−39] For example, in the case of yttrium or gadolinium nitride cluster fullerenes, the [6,6]-monoadduct is the thermodynamically preferred product, while in the case of the smaller scandium and lutetium nitride cluster EMFs, the [5,6]-monoadduct is the thermodynamically preferred product.[37−40]

Since a detailed analysis of the statistically possible number of bisadduct isomers on an I_h-C_{80} cage has not been reported, we present it here, see Figure 1. Assuming that the two addends are identical, and assuming that both [5,6] or [6,6] additions can occur, the total number of statistically possible bisadduct isomers is 91. Of the 91 possible regioisomers, 30 correspond to additions at [5,6]-[5,6]-bonds, 31 to additions at [5,6]-[6,6]-bonds, and 30 to additions at [6,6]-[6,6]-bonds (Figure 1). Of the 30 [5,6]-[5,6]-bisregioisomers, 7 possess a plane of symmetry (C_s-symmetric) and 5 possess a C_2 rotation (C_2-symmetric). Similarly, of the 30 [6,6]-[6,6]-bisregioisomers, 7 are C_s-symmetric and 5 are C_2-symmetric. For the [5,6]-[6,6]-bisregioisomers, only 4 are C_s-symmetric. Of the 91 statistically possible regioisomers, a large majority, 63, possess no symmetry (C_1).

The C_2 symmetric bisadduct regioisomers, if obtained, would possess inherent chirality based on the addition pattern. There are very few examples of chiral endohedral fullerene derivatives, and all of them are chiral because of the presence of asymmetric centers.[41,42]

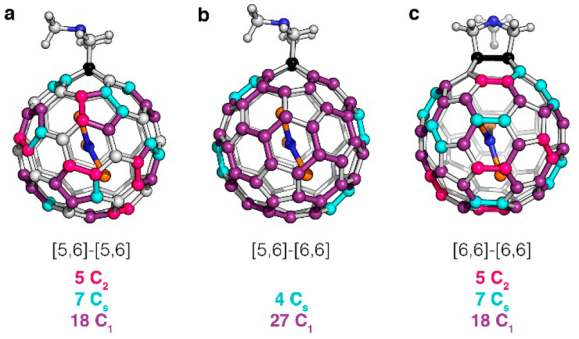

Figure 1. The 91 possible bisadduct regioisomers on an I_h-C_{80} cage. The first pyrrolidine is attached to the bond marked in black: pink bonds denote C_2-symmetric regioisomers, cyan bonds denote C_s-symmetric regioisomers, and purple bonds denote C_1-symmetric regioisomers. (a) [5,6]-[5,6]-bisadducts; (b) [5,6]-[6,6]-bisadducts; (c) [6,6]-[6,6]-bisadducts.

Independent Bisadditions. The reported bis-1,3-dipolar cycloaddition reactions on $M_3N@I_h$-C_{80} (M = Y and Gd) yielded only one NMR-characterized regioisomer.[16] On the basis of NMR spectroscopic experiments and DFT calculations, Yamakoshi et al. assigned the observed isomers to [6,6]-[6,6]-bisadducts, all of which were unsymmetric. Presumably, the [6,6]-[6,6]-bisadduct isomer of $Y_3N@I_h$-C_{80} was converted to an uncharacterized isomeric mixture after thermal treatment, but no details of the specific transformations or characterizations of the new products were provided. Surprisingly, when they used the same reaction conditions with $Sc_3N@I_h$-C_{80} and $Lu_3N@I_h$-C_{80}, they were unable to detect significant amounts of any bisadducts, even when a large excess of *N*-ethylglycine was added.[16] They attributed this behavior to the lower reactivity of the thermodynamically stable [5,6]-monoadduct of $Sc_3N@I_h$-C_{80} and $Lu_3N@I_h$-C_{80}, which in principle are the precursors for the formation of the bisadducts.[16]

In this work, we successfully synthesized and characterized bispyrrolidine adducts of both $Sc_3N@I_h$-C_{80} and $Lu_3N@I_h$-C_{80} for the first time, using similar reaction conditions. Interestingly, most of the bisadducts we purified and characterized exhibit much higher symmetry than the one reported.[16]

Synthesis and Characterization of $Sc_3N@I_h$-C_{80} Bisregioisomers. Bisadducts **1**−**3** were synthesized via the 1,3-dipolar cycloaddition reaction of *N*-ethylglycine and formaldehyde with $Sc_3N@I_h$-C_{80} in *ortho*-dichlorobenzene (*o*-DCB).[43] Bisadducts **1**−**3** were purified using silica gel column chromatography and preparative thin layer chromatography (TLC) in 6%, 13%, and 15% yield, respectively. The matrix-assisted laser desorption/ionization time-of-flight (MALDI-TOF) mass spectra confirmed the presence of $[M + H]^+$ peak for the bisadduct products (*m*/*z* 1252 for all bisadducts **1**−**3**).

The ^{1}H NMR spectrum of bisadduct **1** exhibited 4 AB quartets corresponding to unequivalent methylenes of the two pyrrolidines and two overlapping quartets corresponding to the methylenes of the *N*-ethyl groups (Figure 2a). Therefore, bisadduct **1** is an unsymmetric regioisomer, similar to the one reported for $Y_3N@C_{80}$.[16] Due to the lack of symmetry of bisadduct **1** and the large number of possible C_1-symmetric regioisomers (63), based solely on NMR we cannot assign it to a specific isomer.

DOI: 10.1021/jacs.5b07207
J. Am. Chem. Soc. 2015, 137, 11775−11782

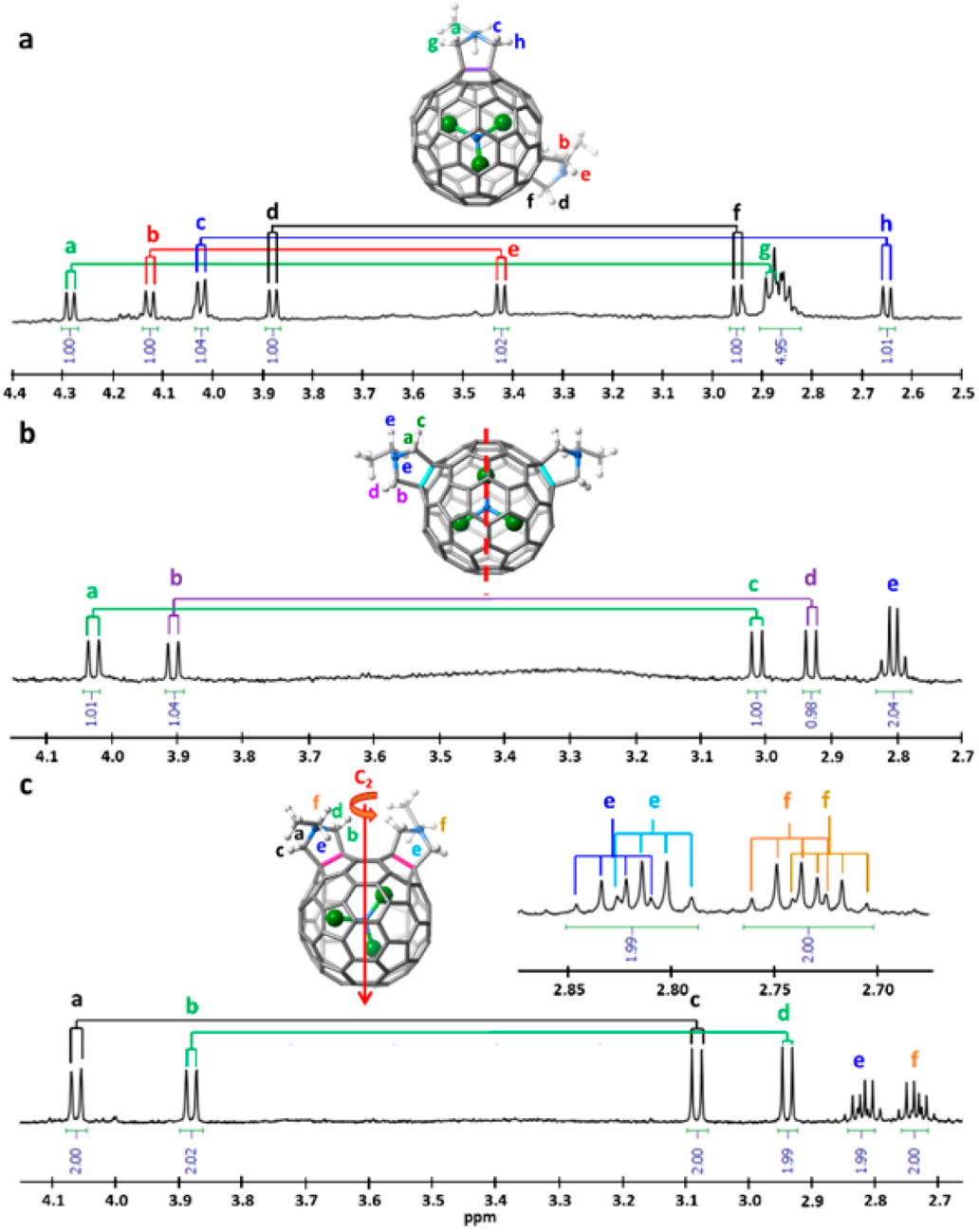

Figure 2. ^{1}H NMR spectrum of (a) bisadduct **1**, (b) bisadduct **2**, (c) bisadduct **3** (600 MHz; $CDCl_3/CS_2$ 1:1, 298 K); assignments based on the observed spectral symmetry, DFT calculations and the ^{1}H−^{1}H COSY NMR spectra, and DFT calculations (see Supporting Information, Figures S12, S16, and S20).

To determine the addition pattern of bisadduct **1**, density functional theory (DFT) full optimizations at the BP86-D_2/TZP(COSMO:o-dCB) level were performed using ADF and the related QUILD computational packages.[44] In principle, all 63 possible C_1-symmetric bisadduct regioisomers should be considered to elucidate the preferred unsymmetric bisadduct. However, the thermodynamic stability of the [5,6]-mono-1,3-dipolar cycloadduct of $Sc_3N@I_h$-C_{80} is higher than that of the [6,6]-monocycloadduct by ca. 8 kcal/mol difference.[45] For these reasons, we only considered [5,6]-[5,6] additions in the case of $Sc_3N@I_h$-C_{80}.[42,43,48,49] In contrast, for $Lu_3N@I_h$-C_{80}, [5,6] and [6,6]-based bisadducts were considered, since the thermodynamic stability of both [5,6]- and [6,6]-adducts are similar.

DFT calculations indicate that the preferred unsymmetrical bisaddition site for $Sc_3N@I_h$-C_{80} corresponds to the bond denoted as 54−72 (Figure 3. The first adduct is always attached to bond 1−5). Many examples reported in the literature show that monopyrrolidines on scandium nitride have the metals far from the addition site.[46−48] Indeed, as observed for the most stable scandium-based [5,6]-monoadduct,[45] the most favorable unsymmetric bisadduct (bond 54−72) has the metal atoms far from the functionalized C−C bonds. The other C_1-symmetric isomers calculated are >1.5 kcal/mol higher in energy than the 54−72 based bisadduct.

The ^{1}H NMR spectrum of bisadduct **2** shows a more symmetric resonance pattern, with two AB quartets corresponding to the methylenes of the pyrrolidines and one quartet

DOI: 10.1021/jacs.5b07207
J. Am. Chem. Soc. 2015, 137, 11775−11782

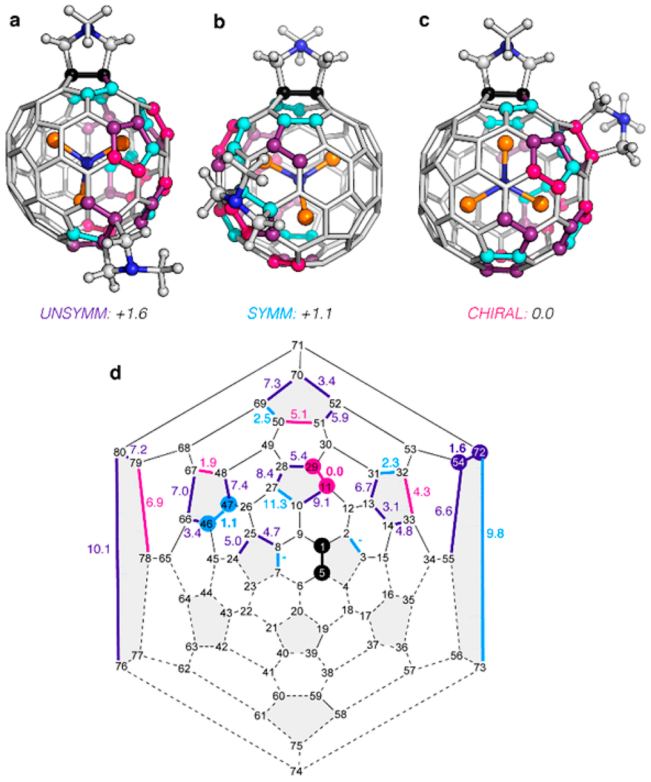

Figure 3. Representation of the most stable Sc-based bisadducts: (a) C_1-symmetric regioisomer on bond 54−72; (b) C_s-symmetric regioisomer on bond 46−47; (c) C_2-symmetric regioisomer on bond 11−29; (d) Schlegel representation of all possible [5,6]-[5,6]-bisadducts and their DFT relative stabilities (in kcal/mol). All possible addition sites are colored according to their symmetry: pink, cyan, and purple for C_2-, C_s-, and C_1-symmetric regioisomers, respectively.

corresponding to the methylenes of the *N*-ethyl groups (Figure 2b). This must be one of the 7 possible symmetric (C_s) [5,6]-[5,6]-regioisomers. DFT calculations of all 7 possible [5,6]-[5,6] C_s-symmetric regioisomers indicated that the preferred second addition site occurs on bond 46−47 (Figure 3b). Again, this structure has the metal atoms far from the functionalized bonds. The second and third most favorable C_s-symmetric bisadducts correspond to bonds 31−32 and 50−69, which are 1.2, and 1.4 kcal/mol less stable, respectively (Figure 3d).

The ^{1}H NMR spectrum of bisadduct **3** exhibits a slightly less symmetric resonance pattern than that of bisadduct **2**, with two AB quartets corresponding to the methylenes of the pyrrolidines and an ABX_3 pattern corresponding to the methylenes of the *N*-ethyl groups (Figure 2c). This ABX_3 pattern is typical of ethyl groups in chiral environments, thus suggesting a C_2-symmetric bisadduct, of which there are only 5 possibilities.[49]

The 5 possible chiral [5,6]-[5,6]-regioisomer structures of $Sc_3N@I_h$-C_{80} were optimized using DFT. The computed relative stabilities of all possible C_2-symmetric bisadducts indicate that the lowest energy corresponds to the second addition at bond 11−29, located close to the initial [5,6]-addition. The other C_2-symmetric bisadducts are ca. > 2 kcal/mol higher in energy. The computed pyramidalization angles for all carbons on the $Sc_3N@I_h$-C_{80} [5,6]-monoadduct revealed that positions 11 and 29 are indeed the most pyramidalized carbons on the fullerene cage. In line with this observation, the deformation energies of the fullerene with respect to the empty fullerene are 30.9 kcal/mol for bisadduct 11−29, whereas it is ca. 37 kcal/mol for the second and third most stable additions. Thus, bisadduct formation at position 11−29 is dramatically favored in the EMF, as the fullerene cage is less distorted.

This C_2-symmetric bisadduct has one of the metal atoms of the Sc_3N cluster directly adjacent to the functionalized [5,6]-bond. This was totally unexpected, since this is usually observed for EMFs containing larger TNT clusters. We performed Energy Decomposition Analysis (EDA) calculations to better rationalize the TNT orientation preference.[50] With the use of the EDA scheme, the total energy of the system is partitioned into a deformation term (the energy required to distort the fragments into the geometry they adopt in the final structure), and an interaction portion, which includes the electrostatic interaction, Pauli repulsion and orbital interaction terms. Empty fullerene structures are taken as the references. Calculations indicate that there exists a correlation between the relative stabilities and both the deformation of the carbon bisadduct cage and the TNT−fullerene interaction energies for bisadduct 11−29. The preferred orientation of the cluster inside the cage actually corresponds to the one possessing the lowest deformation and the largest interaction energy (which mainly results from the orbital interaction term).

The redox potentials of $Sc_3N@I_h$-C_{80} bisadducts **1**−**3** were measured by cyclic voltammetry (CV) in *o*-DCB solutions (Table 1). The CV of bisadducts **1**−**3** exhibited irreversible

Table 1. Redox Potentials (V) of $Sc_3N@I_h$-C_{80} Bisadducts 1−3

compound	$E_{pa}^{+/+2}$	$E_{pa}^{0/+}$	$E_{pc}^{0/-}$	$E_{pc}^{-1/-2}$	$E_{pc}^{-2/-3}$
$Sc_3N@I_h$-C_{80}[46]	1.09	0.59	−1.26	−1.62	−2.37
C_1-[5,6]-[5,6] Bisadduct **1**	0.66	0.02	−1.34	−1.62	−1.80
C_s-[5,6]-[5,6] Bisadduct **2**	0.36	0.15	−1.29	−1.68	-
C_2-[5,6]-[5,6] Bisadduct **3**	0.66	0.05	−1.27	−1.60	−1.79

reduction processes similar to those observed for $Sc_3N@I_h$-C_{80}.[7,11] Unlike the pristine fullerene $Sc_3N@I_h$-C_{80}, bisadducts **1**−**3** showed irreversible oxidation potentials cathodically shifted by approximately 450 mV. Consequently, bisadducts **1**−**3** should exhibit better donor properties and smaller band gap (see Supporting Information).[13]

Synthesis and Characterization of $Lu_3N@I_h$-C_{80} Bisregioisomers. Unexpectedly, when the 1,3-dipolar cycloaddition reaction was done with $Lu_3N@I_h$-C_{80} instead of $Sc_3N@I_h$-C_{80}, only 2 main bisadduct isomers were obtained, bisadducts **4** and **5**, in 7% and 22% yields, respectively. The mass spectra confirmed the presence of $[M + H]^+$ peak for the bisadduct products (m/z 1642 for both bisadducts **4** and **5**).

The ^{1}H NMR spectrum of bisadduct **4** of $Lu_3N@I_h$-C_{80} exhibited a very similar resonance pattern to that of bisadduct **3** of $Sc_3N@I_h$-C_{80}, with two AB quartets corresponding to the methylenes of the pyrrolidines and an ABX_3 system corresponding to the methylenes of the *N*-ethyl groups (Figure 4a). As already discussed, there are only 5 [5,6]-[5,6]-regioisomers out of the 30 possible isomers that can show this chiral (C_2) resonance pattern. Even if hybrid [5,6]-[6,6]-bisadducts were considered, no chiral addition patterns would be possible. [6,6]-[6,6]-Bisadditions could give rise to intrinsically chiral compounds, but these possess much higher energies (see Figure S35E), and thus were not considered based on DFT calculations.

DOI: 10.1021/jacs.5b07207
J. Am. Chem. Soc. 2015, 137, 11775−11782

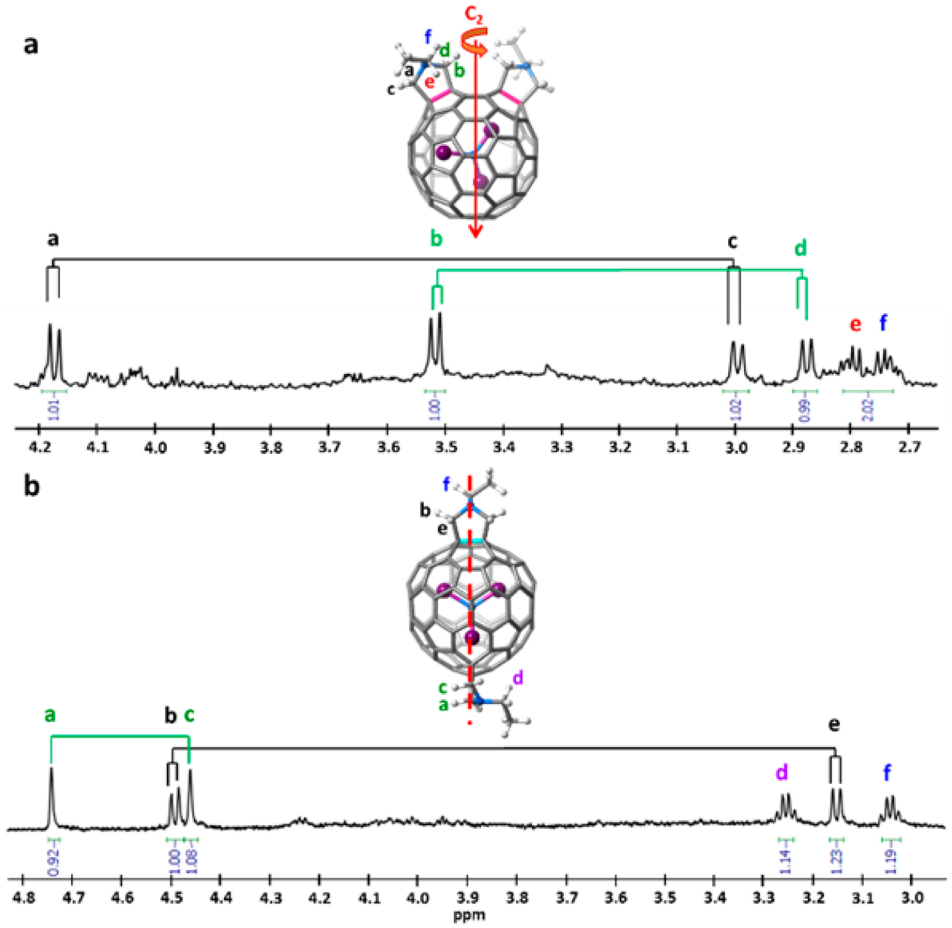

Figure 4. ^{1}H NMR spectrum of (a) bisadduct **4**, and (b) bisadduct **5** (600 MHz; $CDCl_3$/CS2 1:1, 298 K); assignments based on the ^{1}H−^{1}H COSY, ^{1}H−^{1}H NOESY NMR spectra, and DFT calculations (see Supporting Information, Figures S25 and S29).

The 5 possible bis-[5,6]-[5,6]-chiral isomers of $Lu_3N@I_h$-C_{80} were optimized using DFT calculations considering 8 different orientations of the TNT cluster. Not surprisingly, the lowest energy [5,6]-[5,6] C_2-symmetric regioisomer of $Lu_3N@I_h$-C_{80} is the same as for $Sc_3N@I_h$-C_{80} (addition to bond 11−29). This bisadduct is >7 kcal/mol more stable than the other 4 possible C_2-symmetric bisadducts (Figure 5a, 5c).

The ^{1}H NMR spectrum of bisadduct **5** also shows a high degree of symmetry. Since two resonances are uncorrelated singlets at 4.74 and 4.46 ppm (from COSY and NOESY spectra), they cannot correspond to a [5,6]-pyrrolidine addition and must correspond to a [6,6]-pyrrolidine. Furthermore, these two singlets indicate that the second pyrrolidine must be in a position that does not perturb the symmetry of the [6,6]-adduct, and this can only occur by positioning the second pyrrolidine in a relative perpendicular orientation. Similarly, since only one AB quartet is observed, corresponding to the methylenes of the other pyrrolidine, the [6,6]-adduct is not altering the symmetry of the [5,6]-one. Two separate quartets for the methylenes of the *N*-ethyl groups are also observed, confirming that the two pyrrolidines are not symmetrically equivalent (Figure 4b). Exclusively on the basis of the NMR observations, it is possible to assign the structure of this bisadduct to one of only 4 possibilities, all of which exhibit a [5,6]-[6,6]-bisaddition pattern, with mutually perpendicular pyrrolidines. To the best of our knowledge, this is the first mixed (hybrid) bisaddition compound observed for an endohedral system, a rather unanticipated and very interesting result. While the ^{1}H NMR spectrum suggests a very high symmetry, it is also a C_S-symmetric compound.

This unique perpendicular arrangement of the pyrrolidines was confirmed by DFT calculations.

DFT calculations indicate that the most favorable C_s-symmetric bisaddition corresponds to bond 65−78 (Figure 5b,d), leading to a mutually perpendicular bisadduct arrangement. The computed thermodynamic stabilities show that the [5,6]-[5,6] bisadduct **4** (11−29) is 6.7 kcal/mol more stable than the [5,6]-[6,6] **5** (65−78). Linear transit (LT) calculations, i.e., restrained optimization along the reaction coordinate, indicate that the 1,3-dipolar cycloaddition reaction on [6,6]-bonds is kinetically more favored than for [5,6]-additions.[45] This was also observed experimentally by high performance liquid chromatography (HPLC) analysis.[45] Indeed, a thorough investigation of the lowest energy unoccupied molecular orbitals (LUMOs) of $Lu_3N@I_h$-C_{80} demonstrates that bond 65−78 (leading to bisadduct **5**) exhibits LUMO orbital lobes that can effectively interact with the HOMO of the dipole, whereas bond 11−29 (bisadduct **4**) is better aligned to interact via its LUMO + 1 (−3.93 eV), which is 9 kcal/mol higher in energy (Figure 6a). Thus, using Frontier Molecular Orbital (FMO) theory to predict the kinetics of the 1,3-dipolar cycloaddition, we observed that the interaction of the HOMO of the dipole with the LUMO of the monoadduct is ca. 5 kcal/mol more favorable than with the LUMO + 1 (Figure 6a). The fact that bond 65−78 has a properly aligned LUMO orbital to react with the dipole while bond 11−29 has an optimally

DOI: 10.1021/jacs.5b07207
J. Am. Chem. Soc. 2015, 137, 11775−11782

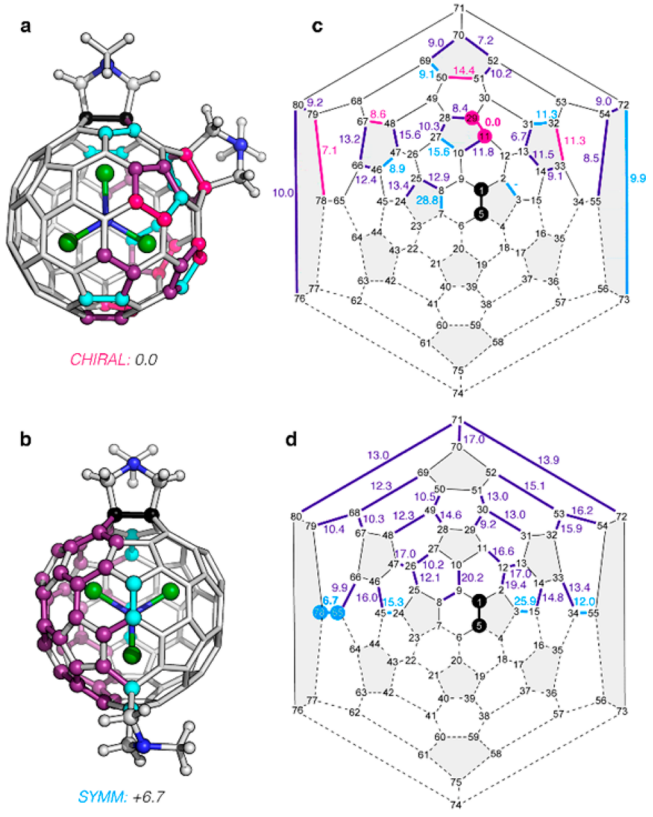

Figure 5. Representation of the most stable Lu-based bisadducts: (a) [5,6]-[5,6] C_2-symmetric regioisomer on bond 11−29, and (b) [5,6]-[6,6] C_s-symmetric on bond 65−78. (c) Schlegel representation of all possible [5,6]-[5,6] and [5,6]-[6,6]-bisadducts and their DFT relative stabilities (in kcal/mol). All possible addition sites are colored according to their symmetry: pink, cyan, and purple for C_2-, C_s-, and C_1-symmetric additions, respectively.

aligned LUMO + 1 explains the higher yield observed experimentally for the former, unambiguously establishing that the addition to bond 65−78 is kinetically preferred.

The computed pyramidalization angles for the $Lu_3N@I_h$-C_{80} [5,6]-monoadduct (Figure 6b) revealed that both 11−29 and 65−78 bonds are more strained. Indeed, 11−29 and 65−78 bisadducts have the lowest deformation energies, indicating that those positions are the most suitable to react in order to release the fullerene strain induced by the presence of the inner Lu_3N moiety. Thus, by analyzing the pyramidalization of the fullerene carbon atoms, the bisaddition pattern can be effectively predicted, indicating that the bisaddition is totally cluster controlled.

The redox potentials of $Lu_3N@I_h$-C_{80} bisadducts **4** and **5** were measured by CV in *o*-DCB solutions (Table 2). The CV of bisadducts **4** and **5** exhibited irreversible reduction processes analogous to those observed for $Lu_3N@I_h$-C_{80}.[7,11] In contrast to $Lu_3N@I_h$-C_{80}, bisadduct **4** showed a cathodic shift of approximately 600 mV and bisadduct **5** of 400 mV. For both cases, irreversible oxidation processes were observed. Therefore, bisadducts **4** and **5** should exhibit better donor properties and smaller band gap values (see Supporting Information).[13]

CONCLUSIONS

We analyzed and described the 91 possible bisaddition regioisomers for an I_h-C_{80} cage based on symmetry (C_1, C_s or C_2-symmetric), assuming identical adducts. We successfully synthesized and characterized the first bisadducts of $Sc_3N@I_h$-C_{80} and $Lu_3N@I_h$-C_{80} using independent, nontethered bis-1,3-dipolar cycloaddition reactions. A very limited number of bisadducts were observed, 3 for $Sc_3N@I_h$-C_{80} and 2 for $Lu_3N@I_h$-C_{80}. Surprisingly, only one of the 5 observed compounds lacks symmetry (C_1), while 2 exhibit C_2 symmetry and 2 others have C_S symmetry, based on ^{1}H NMR analyses. In concert with DFT calculations, it was possible to unambiguously assign the structures of all of the 5 new compounds isolated. The 2 C_2 symmetric compounds are the first intrinsically chiral endohedral fullerenes ever reported, whose chirality arises as a consequence of the intrinsic bisaddition pattern. One of the C_S symmetric compounds, corresponding to a bisadduct of $Lu_3N@C_{80}$, is the first hybrid compound, exhibiting addition of one pyrrolidine on a [5,6]-bond and the other on a [6,6]-bond. DFT calculations were used to rationalize the origins of the differences in regioselectivity observed for scandium and lutetium based bisadducts. This study demonstrates the feasibility of bisadditions to $Sc_3N@C_{80}$ and $Lu_3N@C_{80}$ and establishes that the regiochemistry is more strongly determined/controlled by the endohedral clusters than by the use of exohedrally tethered-controlled bisadducts.

METHODS

Synthesis of $Sc_3N@I_h$-C_{80} Bisregioisomers. To a solution of $Sc_3N@I_h$-C_{80} (6.14 mg, 5.54×10^{-3} mmol, 1 equiv) in 6 mL of *o*-DCB were added *N*-ethylglycine (8.57 mg, 8.31×10^{-2} mmol, 15 equiv) and formaldehyde (8.31 mg, 0.28 mmol, 50 equiv). The reaction mixture was stirred and heated during 15 min at 120 °C under a N_2 atmosphere. The solvent from the reaction mixture was removed under nitrogen, and the crude product was purified by silica gel chromatography using initially CS_2 to elute the unreacted endohedral pristine fullerene, followed by CS_2/$CHCl_3$ 3:2 to elute the monoadduct of $Sc_3N@I_h$-C_{80} (45%) and finally $CHCl_3$/EtOAc 9:1 to elute the bisadducts fraction (38%). Bisadducts **1**, **2**, and **3** were further purified by preparative TLC using $CHCl_3$/EtOAc 9:1 in 6%, 13%, and 15% yield, respectively.

Synthesis of $Lu_3N@I_h$-C_{80} Bisregioisomers. To a solution of $Lu_3N@I_h$-C_{80} (3.52 mg, 2.35×10^{-3} mmol, 1 equiv) in 4 mL of *o*-DCB were added *N*-ethylglycine (3.63 mg, 3.52×10^{-2} mmol, 15 equiv) and formaldehyde (3.52 mg, 0.12 mmol, 50 equiv). The reaction mixture was stirred during 15 min and heated at 120 °C under a N_2 atmosphere. The solvent from the reaction mixture was removed under nitrogen, and the crude product was purified by silica gel chromatography using initially CS_2 to elute the unreacted endohedral pristine fullerene, followed by CS_2:$CHCl_3$ 3:2 to elute the monoadduct of $Lu_3N@I_h$-C_{80} (41%), and finally $CHCl_3$/EtOAc 9:1 to elute the bisadduct **4** (7%) and bisadduct **5** (22%).

Computational Details. Density functional theory (DFT) full optimizations at the ZORA-BP86-D_2/TZP(COSMO:*o*-DCB) level were performed using ADF and the related QUILD computational packages.[44] *N*-Ethyl substituents on the pyrrolidino ring were replaced by methyl groups to reduce the computational complexity of the calculations. Different orientations of the TNT unit were considered in all cases to properly model the TNT unit rotation inside the cage as performed in previous studies.[48,52] All possible 30 [5,6]-[5,6] bisadducts were optimized for $Sc_3N@I_h$-C_{80} considering 8 different orientations of the TNT cluster for the most stable bisadducts, whereas all possible 91 regioisomers with 8 different cluster orientations were optimized for $Lu_3N@I_h$-C_{80} (ca. 800 full BP86-D_2/TZP optimizations). Energy Decomposition Analyses (EDA) were performed as implemented in the ADF computational package.[50] In this EDA scheme, the total energy of the system is divided into

$$\Delta E = \Delta E_{def} + \Delta E_{int}$$

$$\Delta E_{int} = \Delta V_{est} + \Delta E_{Pauli} + \Delta E_{oi} = \Delta E^0 + \Delta E_{oi}$$

DOI: 10.1021/jacs.5b07207
J. Am. Chem. Soc. 2015, 137, 11775−11782

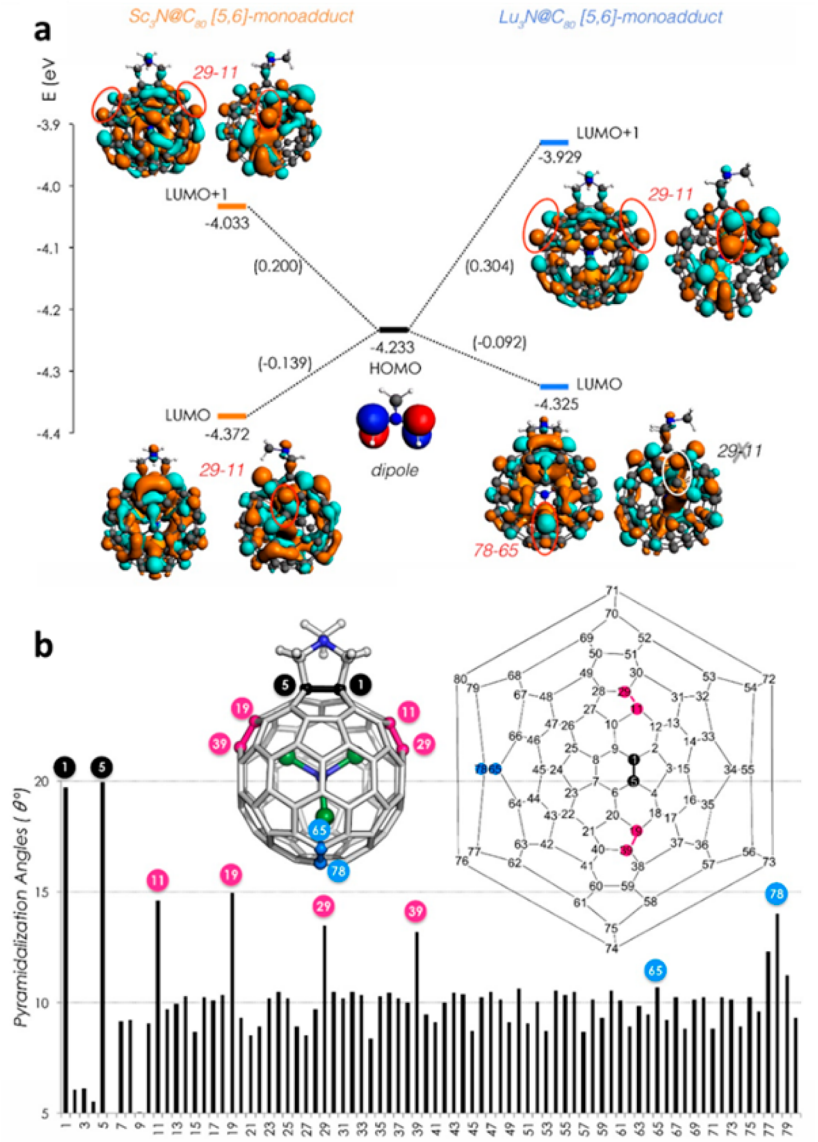

Figure 6. (a) Representation of the LUMO for $Sc_3N@I_h$-C_{80} and $Lu_3N@I_h$-C_{80} and their interaction with the HOMO of the dipole (isosurface value 0.02 au, energies in eV). (b) Representation of the POAV (Pi-Orbital Axis Vector) pyramidalization angle for $Lu_3N@I_h$-C_{80} [5,6]-monoadduct.

Table 2. Redox Potentials (V) of $Lu_3N@I_h$-C_{80} Bisadducts 4 and 5

compound	$E_{pa}^{+/+2}$	$E_{pa}^{0/+}$	$E_{pc}^{0/-}$	$E_{pc}^{-1/-2}$	$E_{pc}^{-2/-3}$
$Lu_3N@I_h$-C_{80}[51]	2.04	0.64	−1.40	-	-
C_2-[5,6]-[5,6] Bisadduct **4**	0.37	0.03	−1.42	−1.74	−2.22
C_s-[5,6]-[6,6] Bisadduct **5**	0.34	0.24	−1.45	−1.81	-

where a deformation term (E_{def}) is the energy required to distort the fragments into the geometry they adopt in the final structure, and an interaction part (E_{int}). The latter includes the electrostatic interaction (V_{elst}), which corresponds to the classical electrostatic interaction between the unperturbed charge distributions of the fragments as they are brought together at the final geometry, Pauli repulsion (E_{Pauli}) comprising the destabilizing interactions between occupied orbitals, and is responsible for any steric repulsion; and orbital interaction (E_{oi}) term that accounts for electron pair bonding, charge transfer, and polarization. Pyramidalization (POAV) angles were computed using POAV3 program (see Supporting Information for complete computational reference list).

Abbreviations. LUMO, low unoccupied molecular orbital; HPLC, high performance liquid chromatography; *o*-DCB, *ortho*-dichlorobenzene; TLC, thin layer chromatography; NMR, nuclear magnetic resonance; COSY, correlation spectroscopy; HMQC, heteronuclear multiple-quantum correlation spectroscopy.

■ ASSOCIATED CONTENT

Supporting Information

The Supporting Information is available free of charge on the ACS Publications website at DOI: 10.1021/jacs.5b07207.

Detailed synthesis and characterization of compounds **1**−**5**, DFT calculations results, and complete computational reference list (PDF)

■ AUTHOR INFORMATION

Corresponding Authors

*silvia.osuna@udg.edu

*echegoyen@utep.edu

Present Address

[‖]M.I.: Department of Organic Chemistry, Universidad Complutense de Madrid, E-28040 Madrid, Spain.

DOI: 10.1021/jacs.5b07207
J. Am. Chem. Soc. 2015, 137, 11775−11782

Author Contributions

[⊥]M.I. and M.G.-B. contributed equally.

Notes

The authors declare no competing financial interest.

■ ACKNOWLEDGMENTS

M.R.C, M.I, S.S.L and L.E. thank the NSF for generous support of this work under the Grant (CHE-1408865). The Robert A. Welch Foundation is also gratefully acknowledged for an endowed chair to L.E. (Grant AH-0033). S.S. thanks the NSF for RUI CHE Grant 1151668. M.G.-B thanks the Spanish MECD for a Ph.D. fellowship (AP2010-2517), and Spanish MINECO for project CTQ2014-52525-P. S.O. thanks the Spanish MINECO CTQ2014-59212-P, Juan de la Cierva Grant (JCI-2012-14438), and the European Community for CIG project (PCIG14-GA-2013-630978). The authors are grateful for the computer resources, technical expertise, and assistance provided by the Barcelona Supercomputing Center - Centro Nacional de Supercomputación.

■ REFERENCES

(1) Kroto, H. W.; Heath, J. R.; O'Brien, S. C.; Curl, R. F.; Smalley, R. E. *Nature* **1985**, *318*, 162.
(2) Heath, J. R.; O'Brien, S. C.; Zhang, Q.; Liu, Y.; Curl, R. F.; Tittel, F. K.; Smalley, R. E. *J. Am. Chem. Soc.* **1985**, *107*, 7779.
(3) Subramoney, S. *Adv. Mater.* **1997**, *9*, 1193.
(4) Kurotobi, K.; Murata, Y. *Science* **2011**, *333*, 613.
(5) Saunders, M.; Jimenez-Vazquez, H. A.; Cross, R. J.; Poreda, R. J. *Science* **1993**, *259*, 1428.
(6) Akasaka, T.; Nagase, S. Endofullerenes: A New Family of Carbon Clusters. In *Developments in Fullerene Science*; Kluwer Academic Publishers: Boston, MA, 2002; Vol. 3.
(7) Chaur, M. N.; Melin, F.; Ortiz, A. L.; Echegoyen, L. *Angew. Chem., Int. Ed.* **2009**, *48*, 7514.
(8) Stevenson, S.; Rice, G.; Glass, T.; Harich, K.; Cromer, F.; Jordan, M. R.; Craft, J.; Hadju, E.; Bible, R.; Olmstead, M. M.; Maitra, K.; Fisher, A. J.; Balch, A. L.; Dorn, H. C. *Nature* **1999**, *402*, 898.
(9) Popov, A. A.; Yang, S.; Dunsch, L. *Chem. Rev.* **2013**, *113*, 5989.
(10) Akasaka, T.; Kato, T.; Kobayashi, K.; Nagase, S.; Yamamoto, K.; Funasaka, H.; Takahashi, T. *Nature* **1995**, *374*, 600.
(11) Izquierdo, M.; Cerón, M. R.; Olmstead, M. M.; Balch, A. L.; Echegoyen, L. *Angew. Chem., Int. Ed.* **2013**, *52*, 11826.
(12) Lu, X.; Bao, L.; Akasaka, T.; Nagase, S. *Chem. Commun.* **2014**, *50*, 14701.
(13) Muqing, C.; Lu, X.; Cerón, M. R.; Izquierdo, M.; Echegoyen, L. In *Endohedral Metallofullerenes*; CRC Press: Boca Raton, FL, 2014; p 173.
(14) Thompson, B. C.; Fréchet, J. M. J. *Angew. Chem., Int. Ed.* **2008**, *47*, 58.
(15) Chen, N.; Ortiz, A. L.; Echegoyen, L. In *Fullerenes: Principles and Applications (2)*; The Royal Society of Chemistry: Cambridge, U.K., 2012; p 12.
(16) Aroua, S.; Garcia-Borràs, M.; Bölter, M. F.; Osuna, S.; Yamakoshi, Y. *J. Am. Chem. Soc.* **2015**, *137*, 58.
(17) You, J.; Dou, L.; Yoshimura, K.; Kato, T.; Ohya, K.; Moriarty, T.; Emery, K.; Chen, C.-C.; Gao, J.; Li, G.; Yang, Y. *Nat. Commun.* **2013**, *4*, 1446.
(18) Chen, W.; Zhang, Q.; Salim, T.; Ekahana, S. A.; Wan, X.; Sum, T. C.; Lam, Y. M.; Hon Huan Cheng, A.; Chen, Y.; Zhang, Q. *Tetrahedron* **2014**, *70*, 6217.
(19) Susarova, D. K.; Goryachev, A. E.; Novikov, D. V.; Dremova, N. N.; Peregudova, S. M.; Razumov, V. F.; Troshin, P. A. *Sol. Energy Mater. Sol. Cells* **2014**, *120*, 30.
(20) Sun, Y.; Cui, C.; Wang, H.; Li, Y. *Adv. Energy Mater.* **2012**, *2*, 966.
(21) Wong, W. W. H.; Subbiah, J.; White, J. M.; Seyler, H.; Zhang, B.; Jones, D. J.; Holmes, A. B. *Chem. Mater.* **2014**, *26*, 1686.
(22) Meng, X.; Zhao, G.; Xu, Q.; Tan, Z. a.; Zhang, Z.; Jiang, L.; Shu, C.; Wang, C.; Li, Y. *Adv. Funct. Mater.* **2014**, *24*, 158.
(23) Kräutler, B.; Müller, T.; Maynollo, J.; Gruber, K.; Kratky, C.; Ochsenbein, P.; Schwarzenbach, D.; Bürgi, H.-B. *Angew. Chem., Int. Ed. Engl.* **1996**, *35*, 1204.
(24) Neti, V. S.; Cerón, M. R.; Duarte-Ruiz, A.; Olmstead, M. M.; Balch, A. L.; Echegoyen, L. *Chem. Commun.* **2014**, *50*, 10584.
(25) Thilgen, C.; Diederich, F. *C. R. Chim.* **2006**, *9*, 868.
(26) Thilgen, C.; Diederich, F. *Chem. Rev.* **2006**, *106*, 5049.
(27) Izquierdo, M.; Cerón, M. R.; Alegret, N.; Metta-Magana, A. J.; Rodriguez-Fortea, A.; Poblet, J. M.; Echegoyen, L. *Angew. Chem., Int. Ed.* **2013**, *52*, 12928.
(28) Hirsch, A.; Brettreich, M. In *Fullerenes*; Wiley-VCH Verlag GmbH & Co. KGaA: Weinheim, 2005; p 289.
(29) Cerón, M. R.; Izquierdo, M.; Pi, Y.; Atehortúa, S. L.; Echegoyen, L. *Chem. - Eur. J.* **2015**, *21*, 7881.
(30) Stevenson, S.; Stephen, R. R.; Amos, T. M.; Cadorette, V. R.; Reid, J. E.; Phillips, J. P. *J. Am. Chem. Soc.* **2005**, *127*, 12776.
(31) Cai, T.; Xu, L.; Shu, C.; Champion, H. A.; Reid, J. E.; Anklin, C.; Anderson, M. R.; Gibson, H. W.; Dorn, H. C. *J. Am. Chem. Soc.* **2008**, *130*, 2136.
(32) Ishitsuka, M. O.; Sano, S.; Enoki, H.; Sato, S.; Nikawa, H.; Tsuchiya, T.; Slanina, Z.; Mizorogi, N.; Liu, M. T. H.; Akasaka, T.; Nagase, S. *J. Am. Chem. Soc.* **2011**, *133*, 7128.
(33) Sawai, K.; Takano, Y.; Izquierdo, M.; Filippone, S.; Martin, N.; Slanina, Z.; Mizorogi, N.; Waelchli, M.; Tsuchiya, T.; Akasaka, T.; Nagase, S. *J. Am. Chem. Soc.* **2011**, *133*, 17746.
(34) Feng, L.; Tsuchiya, T.; Wakahara, T.; Nakahodo, T.; Piao, Q.; Maeda, Y.; Akasaka, T.; Kato, T.; Yoza, K.; Horn, E.; Mizorogi, N.; Nagase, S. *J. Am. Chem. Soc.* **2006**, *128*, 5990.
(35) Lu, X.; Nikawa, H.; Tsuchiya, T.; Maeda, Y.; Ishitsuka, M. O.; Akasaka, T.; Toki, M.; Sawa, H.; Slanina, Z.; Mizorogi, N.; Nagase, S. *Angew. Chem., Int. Ed.* **2008**, *47*, 8642.
(36) Cerón, M. R.; Izquierdo, M.; Aghabali, A.; Valdez, J. A.; Ghiassi, K. B.; Olmstead, M. M.; Balch, A. L.; Wudl, F.; Echegoyen, L. *J. Am. Chem. Soc.* **2015**, *137*, 7502.
(37) Chen, N.; Zhang, E.-Y.; Tan, K.; Wang, C.-R.; Lu, X. *Org. Lett.* **2007**, *9*, 2011.
(38) Cardona, C. M.; Kitaygorodskiy, A.; Echegoyen, L. *J. Am. Chem. Soc.* **2005**, *127*, 10448.
(39) Aroua, S.; Yamakoshi, Y. *J. Am. Chem. Soc.* **2012**, *134*, 20242.
(40) Cerón, M. R.; Li, F.-F.; Echegoyen, L. A. *J. Phys. Org. Chem.* **2014**, *27*, 258.
(41) Maroto, E. E.; Izquierdo, M.; Murata, M.; Filippone, S.; Komatsu, K.; Murata, Y.; Martin, N. *Chem. Commun.* **2014**, *50*, 740.
(42) Maroto, E. E.; Mateos, J.; Garcia-Borràs, M.; Osuna, S.; Filippone, S.; Herranz, M. Á.; Murata, Y.; Solà, M.; Martín, N. *J. Am. Chem. Soc.* **2015**, *137*, 1190.
(43) Cerón, M. R.; Li, F.-F.; Echegoyen, L. *Chem. - Eur. J.* **2013**, *19*, 7410.
(44) Swart, M.; Bickelhaupt, F. M. *J. Comput. Chem.* **2008**, *29*, 724.
(45) Aroua, S.; Garcia-Borràs, M.; Osuna, S.; Yamakoshi, Y. *Chem. - Eur. J.* **2014**, *20*, 14032.
(46) Campanera, J. M.; Bo, C.; Poblet, J. M. *J. Org. Chem.* **2006**, *71*, 46.
(47) Lee, H. M.; Olmstead, M. M.; Iezzi, E.; Duchamp, J. C.; Dorn, H. C.; Balch, A. L. *J. Am. Chem. Soc.* **2002**, *124*, 3494.
(48) Garcia-Borràs, M.; Osuna, S.; Luis, J. M.; Swart, M.; Solà, M. *Chem. - Eur. J.* **2013**, *19*, 14931.
(49) Nelson, G. L.; Williams, E. A. *Prog. Phys. Org. Chem.* **1976**, *12*, 229.
(50) te Velde, G.; Bickelhaupt, F. M.; Baerends, E. J.; Fonseca Guerra, C.; van Gisbergen, S. J. A.; Snijders, J. G.; Ziegler, T. *J. Comput. Chem.* **2001**, *22*, 931.
(51) Cai, T.; Xu, L.; Anderson, M. R.; Ge, Z.; Zuo, T.; Wang, X.; Olmstead, M. M.; Balch, A. L.; Gibson, H. W.; Dorn, H. C. *J. Am. Chem. Soc.* **2006**, *128*, 8581.
(52) Osuna, S.; Valencia, R.; Rodríguez-Fortea, A.; Swart, M.; Solà, M.; Poblet, J. M. *Chem. - Eur. J.* **2012**, *18*, 8944.

DOI: 10.1021/jacs.5b07207
J. Am. Chem. Soc. 2015, 137, 11775−11782